Doctoral Thesis

Search for Multi-Messenger Transients with IceCube and ZTF

Robert Stein

June 25, 2021

Humboldt Universitaet zu Berlin

Colophon
This document was typeset with the help of KOMA-Script and LaTeX using the kaobook class.

The source code of this thesis is available at:
https://github.com/robertdstein/kaobook,
while the scripts used to generate the plots is available at:
https://github.com/robertdstein/thesis_code

The template is a modification of the open-source kaobook class, available at:
https://github.com/fmarotta/kaobook

Publisher
First printed in Oct 2021 by Humboldt Universitaet zu Berlin

A neutrino is not a big thing to be hit by.
In fact it's hard to think of anything much smaller by which one could reasonably hope to be hit. And it's not as if being hit by neutrinos was in itself a particularly unusual event for something the size of the Earth. Far from it. It would be an unusual nanosecond in which the Earth was not hit by several billion passing neutrinos.

–*The Hitchhiker's Guide to The Galaxy*

Preface

writing is hard...

Robert Stein

Abstract

Neutrinos are great, probably

Zusammenfassung

Neutrinos are probably also great auf Deutsch

Contents

List of Figures

List of Tables

An Introduction to Multi-Messenger Astronomy

Neutrino Astronomy with IceCube

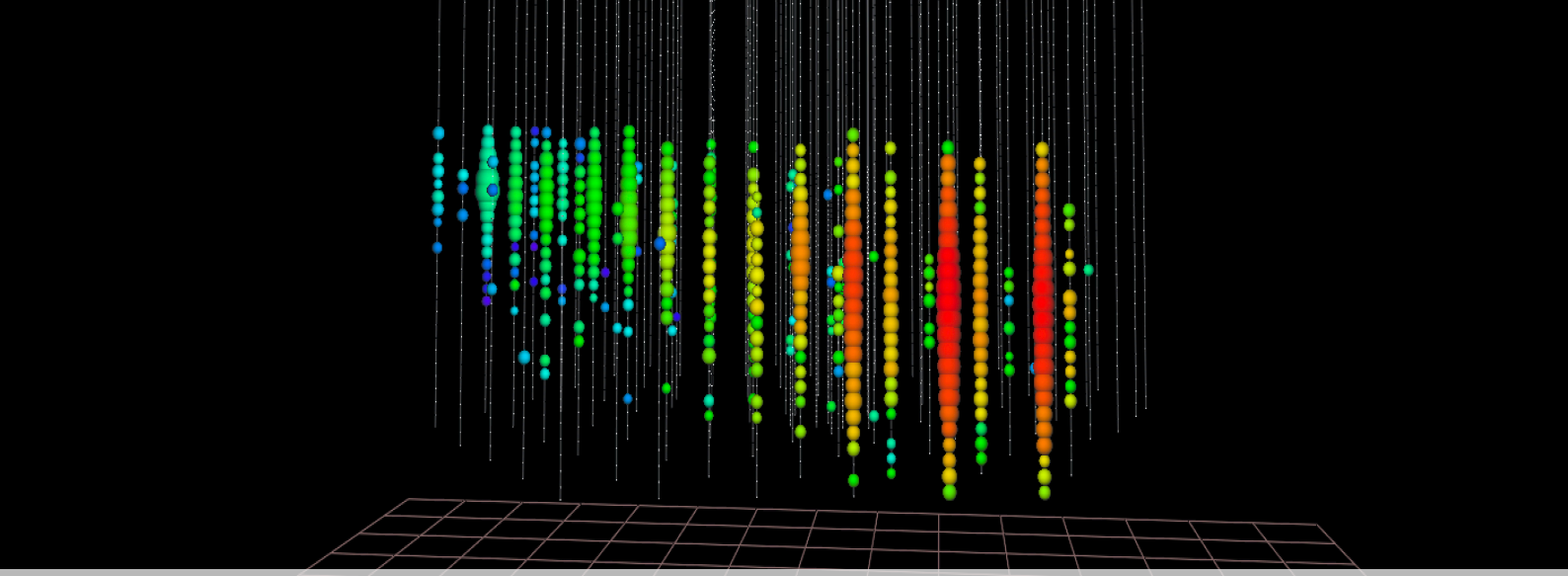

1 IceCube Realtime Alerts

> *A very large part of space-time must be investigated, if reliable results are to be obtained. Otherwise we may (as most English children do) decide that everybody speaks English, and that it is silly to learn French.*

Alan Turing, *Computing Machinery and Intelligence*, 1950

As a complement to the Likelihood analysis methods introduced in Chapter **??**, neutrino astronomy can also be conducted through *realtime* analysis in which automated neutrino alerts are published with low latency. These public neutrino alerts can then be *followed-up* by external observatories, in order to search for possible photon counterparts. This latter aspect is explained in more detail in Chapter 2, where one such follow-up program with the Zwicky Transient Facility (ZTF) is outlined.

In this chapter, the IceCube Realtime Program is introduced. As part of this thesis, the author maintained and further developed the IceCube Realtime System from October 2018 to mid 2020, acting as first responder to the vast majority of neutrino alerts in that period.

1.1 Realtime Multi-Messenger Astronomy

In recent years, there has been a significant interest in the study of transient and variable objects in astronomy (see also Chapter **??**). Driven primarily by the speed at which objects can evolve and disappear, particularly GRBs and latterly Kilonovae, it is often essential that astronomy can be done with minimal latency. In this vein, it is now commonplace for detectors to automatically issue so-called alerts for observations that meet given criteria, to enable other instruments to rapidly obtain near-simultaneous observations. Realtime alerts are automatically issued e.g by GRB-searching instruments such as Swift-BAT and Fermi-GBM, while gravitational-wave events are issued by the LIGO-VIRGO observatories, and high-energy neutrino alerts are issued by IceCube.

These alerts are typically issued via the Gamma-ray Coordination Network (GCN)* system as machine-readable *GCN Notices*, which can then be used to trigger automated telescope scheduling or notification systems. The GCN Notices are then supplemented by *GCN Circulars*†, which are short text summaries of observations that can be rapidly released to the wider astronomy community. GCN circulars are typically sent both by the original observatory and by any observatories which subsequently follow-up the initial detection. For observations of higher community interest, for example detections of potential multi-messenger counterparts, similar text summaries are often shared via the *Astronomer's Telegram* (ATEL) network ‡. These GCN Circulars and ATELs are citeable records of realtime observations, and often form the basis of later peer-reviewed publications.

1.2 The IceCube Realtime System

The IceCube Realtime System has been operating since 2016, providing the first source of high-energy neutrino alerts [1]. The first iteration of the alert system consisted of two streams, namely *High-Energy Starting Events* (HESE) and *Extremely High Energy* (EHE) events. Both EHE [2] and HESE [3] were established event selections used to identify likely-astrophysical neutrinos, which were then adapted to realtime alert selections.

This original system of IceCube alerts continued until May 2019, at which point a new *V2 alert system* was implemented [4]. While the original EHE selection was maintained, the HESE alert selection was improved to reduce the cascade contamination, and improve the astrophysical purity. In addition, a new alert stream based on the *Gamma-ray Follow-Up* (GFU) event selection was initiated [5], with a significantly-elevated rate relative to EHE and HESE alerts. The publication of these three alert streams was unified into a new *IceCube Astrotrack* GCN Notice stream, which was further subdivided into *Gold* and *Bronze* based on the average purity of alerts §. Golden Astrotrack alerts contain an average of 50% astrophysical neutrinos, with the remainder arising from atmospheric background, while Bronze+Gold Astrotrack alerts together have a joint average of 30% astrophysical neutrinos.

As explained in Chapter **??**, filters to identify relevant events are deployed on computers at the South Pole, and detections are flagged with low latency. After fast "online" reconstruction algorithms are applied to events, an automated machine-readable "notice" is distributed via the GCN system. In parallel, data from the event is transmitted via satellite to a computing centre in Madison, Wisconsin where a full likelihood scan is performed on the event.

The alerts are vetted by humans to asses the event quality, with visually inspection being used to confirm classified topology and event recon-

[1]: Aartsen et al. (2017), "The IceCube realtime alert system"

[2]: Aartsen et al. (2016), "Constraints on Ultrahigh-Energy Cosmic-Ray Sources from a Search for Neutrinos above 10 PeV with IceCube"

[3]: Aartsen et al. (2014), "Observation of High-Energy Astrophysical Neutrinos in Three Years of IceCube Data"

[4]: Blaufuss et al. (2019), "The Next Generation of IceCube Real-time Neutrino Alerts"

[5]: Kintscher (2020), "Rapid Response to Extraordinary Events: Transient Neutrino Sources with the IceCube Experiment"

* https://gcn.gsfc.nasa.gov

† https://gcn.gsfc.nasa.gov/gcn3_archive.html

‡ https://www.astronomerstelegram.org/

§ *Silver* alerts were initially reserved for a planned future high-energy cascade stream [5], but this intended naming convention plan appears to have been forgotten because these were ultimately named *IceCube Cascade* alerts

structions. The operating state of the detector is additionally checked. Following these steps, a plain-text GCN circular is distributed to confirm the good nature of the alert, and to provide the updated localisation arising from the full likelihood scan. Each neutrino alert is assigned a unique name with an IceCube detector prefix, the UTC date on which the alert was issued, and a letter denoting the order of alerts on that day (e.g *IC170922A* or *IC190922B*).

1.3 Alert Reconstruction

The standard reconstruction methods introduced in Chapter **??** are generally optimised for large datasets, but for the handful of realtime alert, more computationally-intensive reconstruction methods can be employed. In particular, for multi-messenger counterpart searches the success depends critically on the impact of systematic uncertainties on the localisation, which are not directly accounted for in the likelihood analysis reconstruction methods.

To measure this effect, individual IceCube events can calibrated using *resimulations*. In this approach, many neutrinos are simulated from a similar direction to the reconstructed one of the alert [6]. During the simulation stage, different realisations of systematic uncertainties such as ice properties are randomly chosen, providing an ensemble that corresponds to the limits of knowledge of detector properties. A series of cuts are then applied to select simulated events which 'look similar' to the one observed, accounting for deposited energy, reconstructed direction and stochasticity.

[6]: Pan-Starrs Collaboration et al. (2019), "Search for transient optical counterparts to high-energy IceCube neutrinos with Pan-STARRS1"

Each simulated event is then reconstructed using the same Millipede method as for realtime events, and the best fit position for each simulated event is found. By comparing the difference in log likelihood (LLH) value between the best fit and simulated truth for each event, a histogram can be constructed that describes the PDF of delta LLH value for events similar to a given alert. By combining this information with the LLH landscape for an individual event, the full localisation uncertainty including systematic uncertainty can be derived for that event.

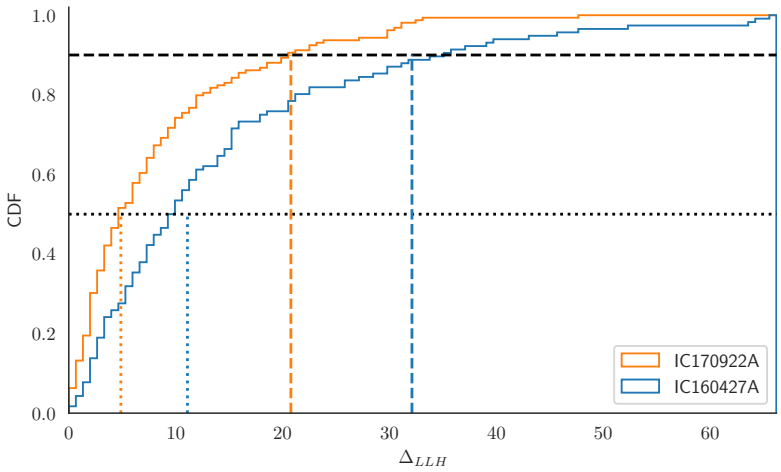

Figure 1.1: Cumulative Distribution Functions (CDFs) for the resimulations of *IC160427A* and *IC170922A*.

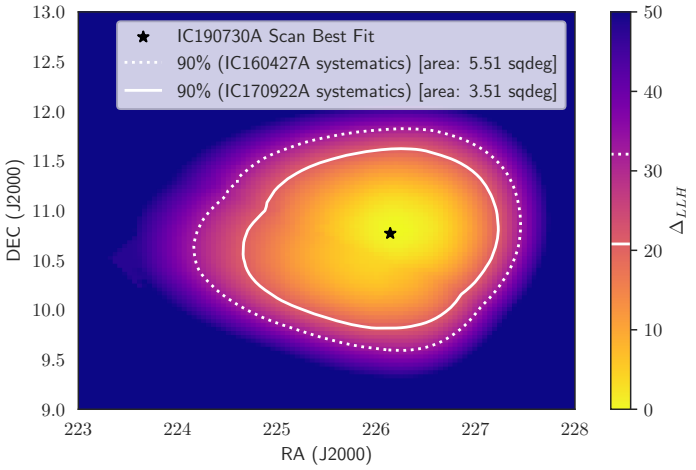

Figure 1.2: An example likelihood contour for *IC190730A*, illustrating both *IC160247A* and *IC170922A* resimulations.

The outcome of resimulations for two alerts, *IC160427A* and *IC170922A*, can be seen as a Cumulative Distribution Function (CDF) in Figure 1.1. 250 resimulated were selected for *IC160427A* ¶, while 159 were selected for *IC170922A*. Dotted lines indicate 50% containment, while dashed lines indicate 90% containment. For *IC160427A* , 50% of resimulated events had an LLH offset between best fit and MC truth of 11.1, and 90% of events within $Delta_{LLH} < 32.1$. By drawing a contour on the likelihood landscape of an alert at $LLH - LLH_{best} = 11.1$ and 32.1, we can say that that the true neutrino arrival direction will lie inside those contours 50% and 90% of the time respectively. In comparison, for *IC170922A*, these critical $Delta_{LLH}$ values are somewhat smaller at 4.9 and 20.8 respectively.

The resimulation process can take many weeks and thousands of CPU hours, so is generally not performed for each new alert. Instead, the outcome of previous resimulations can be used as a rapid solution. At present, all new alerts are issued using the same resimulations from the first public alert (*IC160427A*, see Section 1.5). Additional tailored resimulations are employed in a handful of additional cases, though an effort to perform more comprehensive resimulations is planned. A typical contour is shown in Figure 1.2, for *IC190730A*. The contour inferred from the *IC160247A* resimulation is shown in the solid line, while the *IC170922A* interpretation is dotted.

1.4 Alert Rates

The alert selections are designed based on Monte Carlo simulations, using the recent IceCube measured astrophysical neutrino flux and spectral index of $E^{-2.19}$ as a signal assumption [7]. PDFs are then constructed similar to those in Figure ?? of Chapter ??, calculating signal/background ratios as a function of energy proxy and reconstructed direction, with thresholds then selected such that the integrated background contamination is <70% (for bronze) or <50% (for gold). Each alert is also assigned an individual *signalness* value using the same method, defined as:

[7]: Haack et al. (2017), "A measurement of the diffuse astrophysical muon neutrino flux using eight years of IceCube data."

¶ Of these 250 events, only 117 were available for inclusion in Figure 1.1. The remainder have been tragically lost to the sands of time. This explains the offset in critical values from the CDF for this curve.

Table 1.1: IceCube realtime alert rates.

Alert Selection	Stream Name	Signal Rate [yr^{-1}]	Background Rate [yr^{-1}]	Total Rate [yr^{-1}]
Alerts V1	HESE	1.1	3.7	4.8
	EHE	2.5	1.9	4.4
Alerts V1	**HESE + EHE**	**3.6**	**5.6**	**9.2**
Alerts V2	Gold	6.6	6.1	12.7
	Bronze	2.8	14.7	17.5
Alerts V2	**Gold + Bronze**	**9.4**	**20.8**	**30.2**

$$signalness(E_{reco}|\theta) = \frac{N_{sig}(E \geq E_{reco}|\theta)}{N_{sig}(E \geq E_{reco}|\theta) + N_{bkg}(E \geq E_{reco}|\theta)} \tag{1.1}$$

The alert rates for each stream can be seen in Table 1.1. Under the V1 alert selection, HESE alerts were issued at a rate of 1.1 signal events per year and 3.7 background alerts per year, while EHE alerts were issued at a rate of 2.48 signal alerts per year and 1.91 background alerts per year [1]. For V2, Gold alerts were issued at a rate 12.7 per year, while Bronze alerts were issued at a, additional rate of 17.5 per year, yielding a combing rate of one alert per ~2 weeks [4]. It is clear that the alert rate for V2 is substantially elevated relative to the V1 alert rate.

1.5 Noteworthy IceCube Neutrino Alerts

A summary of all neutrino alerts issued to date is provided in Appendix Table B.1. Individual neutrino alerts of interest are summarised below.

IC160427A

"The PanSTARRS Supernova Neutrino"

The first alert issued under this system, HESE alert *IC160427A* [8], was found to be in spatial coincidence with an optical transient detected by the Pan-STARRS Observatory while following up the alert [6]. This transient, *PS16cgx* was initially tentatively classified as a Type Ic supernova, for which various models have predicted neutrino emission (see Chapter ??). However, the further spectroscopic and photometric evolution indicated that this was more likely a Type Ia Supernova, for which no neutrino emission would be expected.

[8]: Blaufuss (2016), "ICECUBE-160427A neutrino candidate event: updated direction information."

Given that this was the first HESE alert, and the first high-energy neutrino alert for which a possible counterpart was identified, dedicated resimulations of this event were undertaken following the method in Section 1.3. This was the first characterisation of the impact of systematic uncertainties in modelling the polar glacial ice on directional reconstruction with IceCube for high-energy alerts, and the data from this resimulation continue to be used in all new IceCube alerts.

IC170922A

The "TXS 0506+056 Neutrino"

Subsequent neutrino alerts did not yield any probable counterparts, until the detection of EHE alert *IC170922A*‖ [9] in spatial coincidence with flaring blazar TXS 0506+056 [10]. After accounting for trial correction from historical neutrino alerts, a chance coincidence was disfavoured at the 3σ level [11]. The event was also resimulated in the same manner as *IC160427A* . Remarkably, despite its radically-different topology of through-going muon rather than starting track, the results were found to be broadly consistent. More details of TXS 0506+056 are given in Section **??**.

[9]: Kopper et al. (2017), "IceCube-170922A - IceCube observation of a high-energy neutrino candidate event."

[10]: Tanaka et al. (2017), "Fermi-LAT detection of increased gamma-ray activity of TXS 0506+056, located inside the IceCube-170922A error region."

[11]: IceCube Collaboration et al. (2018), "Multimessenger observations of a flaring blazar coincident with high-energy neutrino IceCube-170922A"

IC190331A

The"Multi-PeV neutrino"

A starting track was observed on 2019 March 30th [12], with a deposited energy of ~5.3 PeV. The initial reconstruction based on *SplineMPE* was inaccurate (for the reasons outlined in Chapter **??**., but the update Millipede reconstruction yielded a well-localised position of ~1 sq. deg. on the sky. Given the extraordinarily high deposited energy, and the downgoing starting track topology which disfavours any atmospheric origin (see Chapter **??**), IC190331A was one of a handful of track alerts for which an astrophysical origin can be reasonably described as 'highly likely'.

[12]: Kopper (2019), "IceCube-190331A - IceCube observation of a high-energy neutrino candidate event."

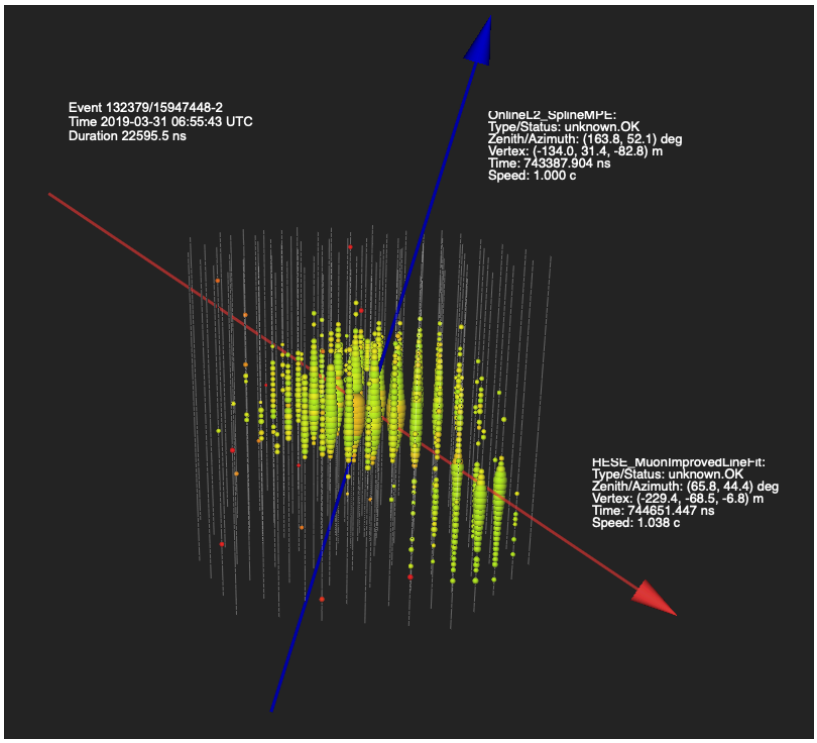

Figure 1.3: Event view of IC190331A. Credit: Cristina Lagunas Gualda

‖ alternatively named *'The neutrino that launched one thousand telecons'* (Credit: E. Blaufuss)

IC190730A

The "ICRC neutrino"

IC190730A was a golden neutrino alert with a signalness of 67% [13], which arrived in the middle of the neutrino astronomy session of the 36th *International Cosmic Ray Conference* (ICRC). Following the automated notice, the full likelihood reconstruction clearly showed it was well-localised, and spatially coincident with FSRQ *PKS 1502+106* (see Chapter **??**). This particular blazar is extremely bright, being 15th brightest in the sky in terms of integrated gamma-ray energy flux, and owing to its high redshift of z=1.84, is one of the most luminous known blazars [14]. This coincidence was reported in the corresponding GCN circular, and triggered a broad multi-wavelength follow-up campaign.

[13]: Stein (2019), "IceCube-190730A - IceCube observation of a high-energy neutrino candidate event"

[14]: Franckowiak et al. (2020), "Patterns in the Multiwavelength Behavior of Candidate Neutrino Blazars"

Though blazar was not found to be flaring in gamma-rays at short timescales [14], OVRO reported that the radio flux was in recent months elevated relative to the decade long observation baseline [15]. Similar behaviour has been claimed for *TXS 0506+056*, and other neutrino-coincident blazars [15]. Comprehensive time-dependent modelling has found that the detection of a neutrino alert from *PKS 1502+106* is consistent with the multi-wavelength observations of this object, so a neutrino-blazar association is plausible [16].

[15]: Kiehlmann et al. (2019), "Neutrino candidate source FSRQ PKS 1502+106 at highest flux density at 15 GHz"

[16]: Rodrigues et al. (2021), "Multiwavelength and Neutrino Emission from Blazar PKS 1502 + 106"

IC190922B

The "SN2019pqh neutrino"

On 2019 September 22nd, IceCube for the first time reported multiple high-energy neutrino alerts on a single day. The latter of these was *IC190922B*, a gold alert with a reported signalness of 50.5% [17]. Follow-up observations of this alert were undertaken by the author with the Zwicky Transient Facility (ZTF), as part of a dedicated neutrino follow-up program introduced in Chapter 2.

[17]: Blaufuss (2019), "IceCube-190922B - IceCube observation of a high-energy neutrino candidate event"

One candidate supernova was found, *SN2019pqh*, in spatial and temporal coincidence with the alert [18]. Unlike PS16cgx, this was the first young supernova reported in spatial coincidence with a high-energy neutrino which would be compatible with the CSM-Interaction model introduced in Chapter **??**. However, as explained in Section 2.2, further spectroscopic observations ultimately disfavoured the association.

[18]: Stein et al. (2019), "A candidate supernova coincident with IceCube-190922B from ZTF"

IC191001A

The "Bran Stark neutrino"

A high-energy gold neutrino event was detected on 2019 October 10, with an estimated signalness of 59% [19]. A bright Tidal Disruption Event (TDE) *AT2019dsg* was found by the author in spatial coincidence with this alert [20], as part of follow-up observations using ZTF. This neu-

[19]: Stein (2019), "IceCube-191001A - IceCube observation of a high-energy neutrino candidate event"

[20]: Stein et al. (2021), "A tidal disruption event coincident with a high-energy neutrino"

trino is explained in much greater detail in Chapter **??**. As with all ZTF-detected TDEs, AT2019dsg was assigned a nickname inspired by once-popular HBO series *Game of Thrones*, in this case named after character *Bran Stark* [21].

[21]: van Velzen et al. (2020), "Seventeen Tidal Disruption Events from the First Half of ZTF Survey Observations: Entering a New Era of Population Studies"

IC200107A

The"Flaring extreme blazar neutrino"

IC200107A was a high-energy neutrino which passed the initial HESE event selection, but did not qualify as a gold or bronze astrotrack event due to a possible cascade classification [22]. However, visual inspection of the event suggested a starting-track topology, which was confirmed by a dedicated Neutral Network topology classifier [23]. A GCN circular was thus issued to publicise the neutrino arrival direction. However, given the extraordinary nature of the neutrino selection, no signalness estimate was provided.

[22]: Stein (2020), "IceCube-200107A: IceCube observation of a high-energy neutrino candidate event"

[23]: Kronmueller et al. (2019), "Application of Deep Neural Networks to Event Type Classification in IceCube"

Two gamma-ray detected blazars were found within the neutrino localisation, *4FGL J0955.1+3551* and *4FGL J0957.8+3423*. The latter of these was not significantly detected at the time of neutrino detection, nor was there any evidence of flaring activity contemporaneous with the neutrino detection. The other blazar *4FGL J0955.1+3551* (also known as *BZB J0955+3551* and *3HSP J095507.9+355101*) belongs to the specific subclass of *extreme blazars*, which are characterised be synchrotron peaks at very high-frequencies, which had been proposed as especially promising candidates of high-energy neutrinos [24]. Follow-up observations by *Swift*-XRT of the source revealed a dramatic simultaneous X-ray flare [25, 26], of particular interest because of the importance of X-ray photons in the $p\gamma$ neutrino production models introduced in Chapter **??**.

[24]: Padovani et al. (2016), "Extreme blazars as counterparts of IceCube astrophysical neutrinos"

[25]: Krauss et al. (2020), "Swift follow-up observations of IceCube-200107A: Identification of a X-ray high state for 4FGL J0955.1+3551"

[26]: Giommi et al. (2020), "Swift observation of a flaring very extreme blazar in the error region of the high-energy neutrino Ice-Cube 200107A"

More comprehensive multi-frequency modelling has confirmed that the detection of a neutrino alert from an extreme blazar is realistic, though the simultaneous X-ray flare may not be directly related to neutrino production [27–29]. The probability for chance coincidence of the neutrino alert with an extreme blazar flaring in X-rays was calculated by the author of this thesis to be 3.7×10^{-3}, but in the absence of any systematic X-ray blazar follow-up program it is unclear how this number could be trial corrected (see Chapter **??**) [27]. The statistical evidence for this association is thus insufficient to draw any definitive conclusions about the neutrino origin.

[27]: Paliya et al. (2020), "Multifrequency Observations of the Candidate Neutrino-emitting Blazar BZB J0955+3551"

[28]: Giommi et al. (2020), "3HSP J095507.9+355101: A flaring extreme blazar coincident in space and time with IceCube-200107A"

[29]: Petropoulou et al. (2020), "Comprehensive Multimessenger Modeling of the Extreme Blazar 3HSP J095507.9+355101 and Predictions for IceCube"

IC200530A

The "Tywin Lannister neutrino"

IC200530A was a high-energy gold alert detected on 2020 May 30th, with a signalness estimate of 59% [30]. The neutrino was also observed as part of the ZTF neutrino follow-up program, and the bright nuclear flare *AT2019fdr* was identified by the author as a probable optical counterpart [31]. The object was later classified as a likely TDE [32], the second found in spatial and temporal coincidence with a high-energy neutrino. More

[30]: Stein (2020), "IceCube-200530A: IceCube observation of a high-energy neutrino candidate event"

[31]: Reusch et al. (2020), "IceCube-200530A: Candidate Counterparts from the Zwicky Transient Facility"

[32]: Frederick et al. (2020), "A Family Tree of Optical Transients from Narrow-Line Seyfert 1 Galaxies"

details on this object are given in Section 2.2. The ZTF-assigned Game of Thrones name was *Tywin Lannister*.

Optical follow-up with ZTF

2 Transient Follow-up with ZTF

> *We are all in the gutter, but some of us are looking at the stars*
>
> Oscar Wilde, *Lady Windermere's Fan*, 18??

The motivation for all real-time analysis and prompt follow-up observations of external triggers is to obtain contemporaneous data. Put another way, these observations are designed to quickly identify time-dependent transient or variable activity which would be missed by untargeted survey operations. In the case of GW and short GRB follow-up, searches are targeted towards identifying kilonovae (KNe), of which GW170817/AT2017gfo was a spectacular well-documented first example. These KNe are inherently fast-evolving transients which will by definition not be present before the extrenal trigger. For neutrinos, there are a proliferation of possible optical transients (e.g GRBs, TDEs, SNe) and variable objects (primarily blazars) which could be identified in an optical follow-up observations. In both cases, a handful of potentially interesting extragalactic objects will need to be selected against a vast background of spurious detections, and unrelated galactic or solar-system objects.

2.1 The Ampel Follow-up Pipeline

Given the similar challenge, a single flexible analysis, the *Ampel Follow-up Pipeline*, was developed by the author to identify candidate counterparts to GW, GRB and neutrino trigger events. ZTF is particularly well-suited to this type of extragalactic transient discovery, because ZTF routinely images the visible Northern Sky once every three nights to a median depth of 20.5^m as part of a public survey [33]. This provides an

[33]: Bellm et al. (2019), "The Zwicky Transient Facility: Surveys and Scheduler"

extensive base to distinguish between new transients that could be coincident with an external trigger, and those with previous detections. The large volumetric survey speed of ZTF often provides significant serendipitous coverage of events. This wide-field cadence can however be supplemented by dedicated Target-of-Opportunity (ToO) observations scheduled for a particular trigger through the GROWTH ToO Marshal [34].

[34]: Coughlin et al. (2019), "2900 Square Degree Search for the Optical Counterpart of Short Gamma-Ray Burst GRB 180523B with the Zwicky Transient Facility"

As introduced in Chapter **??**, all ZTF science images are processed, significant detections are extracted, and these are archived in a database at DESY as part of the local computer infrastructure (the *archive database*). External triggers, which come in the form of probability skymaps or GCN circulars, are downloaded and parsed with *Ampel Follow-up Pipeline*. The archive database is then queried for coincident alerts, using either temporal indexing or spatial indexing depending on the size of the target region. Once loaded, these alerts are then filtered by the *Ampel Follow-up Pipeline* using *AMPEL* [35], a platform for realtime analysis of multi-messenger astronomy data. Our selection is based on an algorithm for identifying extragalactic transients [35]. In order to identify candidate counterparts, we apply the following cuts to ToO and survey data:

[35]: Nordin et al. (2019), "Transient processing and analysis using AMPEL: alert management, photometry, and evaluation of light curves"

- We reject likely subtraction artefacts using machine learning classification and morphology cuts [36]. Subtractions must be positive, i.e a candidate must be brighter than the same position in stacked reference images.
- We reject solar system objects through matches to known catalogues [36]. We further remove uncatalogued solar system objects by requiring multiple detections for each candidate at the same location, separated temporally by at least 15 minutes, thereby rejecting moving objects.
- We reject galactic stellar sources by removing detections cross-matched to objects with measured parallax in the second data release of the *GAIA* satellite [37]. Objects are rejected if they have non-zero parallax with a significance of at least 3σ. We further reject likely stars with machine learning classifications, based on sources detected by Pan-STARRS1 [38], removing those objects with an estimated stellar probability greater than 80%.
- We reject AGN variability by cross-matching objects to the WISE survey. We identify likely AGN by applying a series of cuts based on measured IR colour [39].
- We rejected unassociated objects by requiring both spatial and temporal coincidence with a given trigger.

[36]: Mahabal et al. (2019), "Machine Learning for the Zwicky Transient Facility"

[37]: Gaia Collaboration et al. (2018), "Gaia Data Release 2. Summary of the contents and survey properties"

[38]: Tachibana et al. (2018), "A Morphological Classification Model to Identify Unresolved PanSTARRS1 Sources: Application in the ZTF Real-time Pipeline"

[39]: Wright et al. (2010), "The Wide-field Infrared Survey Explorer (WISE): Mission Description and Initial On-orbit Performance"

These cuts typically yield ~0.2 candidates per square degree of sky. Promising candidates are prioritised for spectroscopic classification, to confirm or rule out a possible association with a given neutrino.

2.2 Neutrino Follow-up Program

ZTF has since its inception had a dedicated program to identify sources of high-energy astrophysical neutrinos, through targeted follow-up observations. A significant component of this thesis was the initial development and operation of this neutrino follow-up program. Given the

proliferation of proposed source classes, neutrino follow-up are characterised by searching relatively well-localised regions for poorly-defined objects. This is particularly true for optical follow-up, where potential counterparts include Tidal Disruption Events (TDEs), Type IIn or choked jet SNe, kilonovae, GRB afterglows, superluminous supernovae (SLSNe) or blazar flares (see Chapter **??** for a comprehensive list). While pre-neutrino detections could rule out neutrino production from choked jet supernovae, in most cases we do not even have stringent constraints in when neutrinos may be expected.

For neutrinos, spatial and temporal coincidence is ensured by requiring that an object lies within the reported 90% localisation rectangle from IceCube, and being detected at least once following the neutrino arrival time. We have followed up N neutrinos in the period from survey start on 2018 March 20 to 2020 June 31, out of a total of N neutrino alerts published by IceCube. Table 2.2 summarises each neutrino alert that has been observed by ZTF. From 2019 June 17, IceCube published neutrino alerts with improved selection criteria to provide an elevated alert rate [4] (see Chapter 1 for more details). In addition to 1 of the 12 alerts under the old V1 selection, ZTF followed up 7 of the 19 alerts published under the V2 selection. In general, we aim to follow all well-localised neutrinos of likely astrophysical origin reported by IceCube which are visible to ZTF and can be observed promptly.

[4]: Blaufuss et al. (2019), "The Next Generation of IceCube Real-time Neutrino Alerts"

Those alerts not observed by ZTF are summarised in Table 2.4. Of those 23 alerts not followed up by ZTF, the primary reasons were proximity to the Sun (8/23), alerts with poor localisation and low astrophysical probability (6/23) and alert retraction (4/23). For events which were reported with estimates of astrophysical probability, we chose not to follow up those that had both low astrophysical probability ($< 50\%$) and large localisation regions (> 10 sq. deg.). This value was not reported for high-energy starting events (HESE) under the old IceCube alert selection, nor for one alert, IC200107A, that was identified outside of the standard alert criteria [22] (see also Chapter 1). The full breakdown of neutrino observations statistics can be seen in Figure N.

[22]: Stein (2020), "IceCube-200107A: IceCube observation of a high-energy neutrino candidate event"

Each neutrino localisation region can typically be covered by one or two ZTF observation fields. Multiple observations are scheduled for each field, with both *g* and *r* filters, and a separation of at least 15 minutes between images. These observations typically last for 300 s, with a typical limiting magnitude of 21.0^m. ToO observations are typically conducted on the first two nights following a neutrino alert, before swapping to serendipitous coverage as part of the public survey.

MENTION THAT COMMISSIONING ONE

)

AT2019fdr

ZTF serendipitously observed the localisation of neutrino IC200530A just 10 minutes after detection, as part of routine survey operations [30]. Additional ToO observations were then conducted on 2020 May 31 in g- and r-band, and again on 2020 June 1. At this point AT2019fdr was identified by the pipeline as a candidate neutrino source [31]. The transient

[30]: Stein (2020), "IceCube-200530A: IceCube observation of a high-energy neutrino candidate event"

[31]: Reusch et al. (2020), "IceCube-200530A: Candidate Counterparts from the Zwicky Transient Facility"

Table 2.1: Summary of the eight neutrino alerts followed up by ZTF. IC191001A is highlighted in bold. The 90% area column indicates the region of sky observed at least twice by ZTF, within the reported 90% localisation, and accounting for chip gaps. The *signalness* estimates the probability that each neutrino is of astrophysical origin, rather than arising from atmospheric backgrounds.

Event	R.A. (J2000) (deg)	Dec (J2000) (deg)	90% area (sq. deg.)	ZTF obs (sq. deg.)	Signalness	Ref
IC190503A	120.28	+6.35	1.94	1.37	36%	[40, 41]
IC190619A	343.26	+10.73	27.16	21.57	55%	[42, 43]
IC190730A	225.79	+10.47	5.41	4.52	67%	[13, 44]
IC190922B	5.76	-1.57	4.48	4.09	51%	[17, 18, 45]
IC191001A	**314.08**	**+12.94**	**25.53**	**20.56**	**59%**	**[19, 46, 47]**
IC200107A	148.18	+35.46	7.62	6.22	-	[22, 48]
IC200109A	164.49	+11.87	22.52	20.06	77%	[49, 50]
IC200117A	116.24	+29.14	2.86	2.66	38%	[51–53]

Table 2.2: Summary of the 21 neutrino alerts followed up by ZTF since survey start on 2018 March 20.

Event	R.A. (J2000) [deg]	Dec (J2000) [deg]	90% area [sq. deg.]	ZTF obs [sq. deg.]	Signalness	Ref
IC190503A	120.28	+6.35	1.9	1.4	36%	[40, 41]
IC190619A	343.26	+10.73	27.2	21.6	55%	[42, 43]
IC190730A	225.79	+10.47	5.4	4.5	67%	[13, 44]
IC190922B	5.76	-1.57	4.5	4.1	51%	[17, 45]
IC191001A	314.08	+12.94	25.5	20.6	59%	[19, 47]
IC200107A	148.18	+35.46	7.6	6.2	-	[22, 48]
IC200109A	164.49	+11.87	22.5	20.1	77%	[49, 50]
IC200117A	116.24	+29.14	2.9	2.7	38%	[**ic200117a_ztf2**, 51, 52]
IC200512A	295.18	+15.79	9.8	9.3	32%	[**ic200512a_ztf**, 54]
IC200530A	255.37	+26.61	25.3	22.0	59%	[**ic200530a_ztf2**, 30, 31]
IC200620A	162.11	+11.95	1.7	1.2	32%	[**ic200620a_ztf**, 55]
IC200916A	109.78	+14.36	4.2	3.6	32%	[**ic200916a**, **ic200916a_ztf**, **ic200916a_ztf**
IC200926A	96.46	-4.33	1.7	1.3	44%	[**ic200926a**, **ic200926a_ztf**]
IC200929A	29.53	+3.47	1.1	0.9	47%	[**ic200929a**, **ic200929a_ztf**]
IC201007A	265.17	+5.34	0.6	0.5	88%	[**ic201007a**, **ic201007a_ztf**]
IC201021A	260.82	+14.55	6.9	6.3	30%	[**ic201021a**, **ic201021a_ztf**]
IC201130A	30.54	-12.10	5.4	4.5	15%	[**ic201130a**, **ic201130a_ztf**]
IC201209A	6.86	-9.25	4.7	3.2	19%	[**ic201209a**, **ic201209a_ztf**]
IC201222A	206.37	+13.44	1.5	1.0	53%	[**ic201222a**, **ic201222a_ztf**]
IC210210A	206.06	+4.78	2.8	2.1	65%	[**ic210210a**, **ic210210a_ztf**]
IC210510A	268.42	+3.81	4.0	4.0	28%	[**ic210510a**, **ic210510a_ztf**]

Table 2.3: Summary of the 23 neutrino alerts that were not followed up by ZTF since survey start on 2018 March 20. Of these, 4/23 were retracted, 11/23 were inaccessible to ZTF for various reasons, 6/23 were deemed alerts of poor quality, while just 2/23 were alerts that were missed although they passed our criteria.

Cause	Events
Alert Retraction	IC180423A[56], IC181031A[57], IC190205A[58], IC190529A[59]
Proximity to Sun	IC180908A[60], IC181014A[61], IC190124A[62], IC190704A[63] IC190712A[64], IC190819A[65], IC191119A[66], IC200227A[67]
Low Altitude	IC191215A[68]
Southern Sky	IC190331A[12], IC190504A[69]
Poor Signalness & Localisation	IC190221A[70], IC190629A[71], IC190922A[72] IC191122A[73], IC191204A[74], IC191231A[75]
Bad Weather	IC200120A[76, 77]
Telescope Maintenance	IC181023A[78]

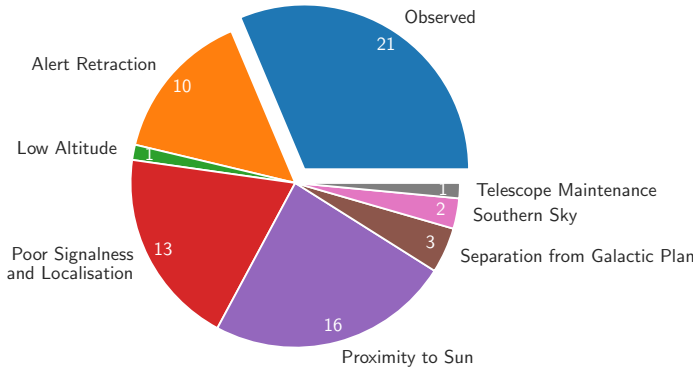

Figure 2.1: Breakdown of the neutrino follow-up program, as of 2021 June 25.

Table 2.4: Summary of the 46 neutrino alerts that were not followed up by ZTF since survey start on 2018 March 20.

Cause	Events
Alert Retraction	IC180423A [56], IC181031A [57], IC190205A [58], IC190529A [59]
	IC200120A [76], IC200728A [**ic200728a**], IC201115B [**ic201115b**], IC210213A [**ic210**
	IC210322A [**ic210322a**], IC210519A [**ic210519a**]
Proximity to Sun	IC180908A [60], IC181014A [61], IC190124A [62], IC190704A [63]
	IC190712A [64], IC190819A [65], IC191119A [66], IC200227A [67]
	IC200421A [79], IC200615A [80], IC200806A [**ic200806a**], IC200921A [**ic200921**
	IC200926B [**ic200926b**], IC201014A [**ic201014a**], IC201115A [**ic201115a**], IC201221A [**i**
Low Altitude	IC191215A [68]
Southern Sky	IC190331A [12], IC190504A [69]
Separation from Galactic Plane	IC201114A [**ic201114a**], IC201120A [**ic201120a**], IC210516A [**ic210516a**]
Poor Signalness and Localisation	IC190221A [70], IC190629A [71], IC190922A [72], IC191122A [73]
	IC191204A [74], IC191231A [75], IC200410A [81], IC200425A [82]
	IC200523A [83], IC200614A [84], IC200911A [**ic200911a**], IC210503A [**ic210503**
	IC210608A [**ic210608a**]
Telescope Maintenance	IC181023A [78]

AT2019fdr had originally been discovered by ZTF on 2019 May 03 [85], but remained in a significantly-elevated flux state at the time of neutrino detection (see Figure 2.2).

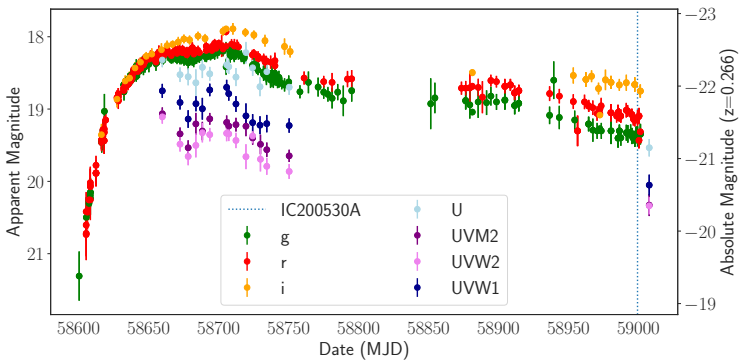

Figure 2.2: ZTF lightcurve of AT2019fdr, with observations in g, r and i band.

A spectrum of the object was taken on 2019 June 8, which gave an ambiguous classification but found a redshift of 0.267 on the basis of nebular emission lines (see Figure 2.3). Given the consistency of the transient po-

sition with the host nucleus, and the bright nature of transient, there was initially considerable interest in this object as a possible TDE or superluminous supernova (SLSN). As can be seen in Figure 2.2, the transient peaked at an absolute magnitude of -22.8 in i-band, with little apparent fading through to the detection of the neutrino 10 months later.

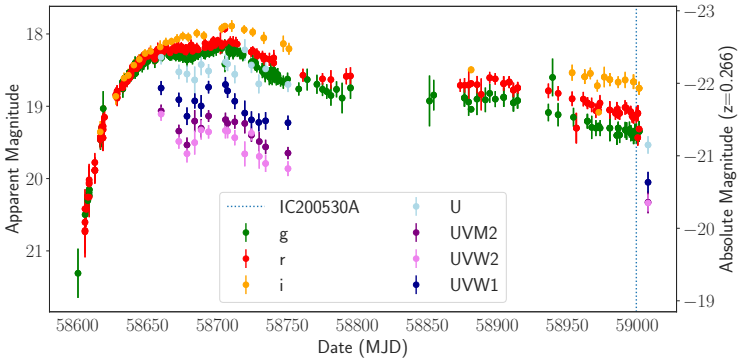

Figure 2.3: ZTF lightcurve of AT2019fdr, with observations in g, r and i band.

The object was tentatively classified as a luminous Type IIn supernova, though the possibility of an AGN classification was also mentioned [86]. Given the lack of temperature evolution over the subsequent 10 months of observation, a supernova classification seems unlikely. Instead, AT2019fdr more likely belongs to a recently-identified class of flares in Narrow-line Seyfert galaxies [87]. Indeed, our late-time spectroscopy (Figure 2.3) reveals iron emission lines characteristic of these flares.

[87]: Trakhtenbrot et al. (2019), "A new class of flares from accreting supermassive black holes"

Flares that fall into the spectroscopic class defined by [87] all occurred in Narrow-Line Seyfert 1 (NLS1) galaxies. They show a large long-duration flare which leads to a sustained flux increase on timescales of many months, with little apparent temperature or color evolution. Such flares also have characteristic spectroscopic features, namely emission lines at λ4640 and λ4686 as well as an OIII-complex, which distinguish them from other objects. These signatures are also present for AT2019fdr (red and blue lines in Figure 2.3).

[87]: Trakhtenbrot et al. (2019), "A new class of flares from accreting supermassive black holes"

To date, ZTF has identified 5 large outburst from NLS1's. Accounting for all neutrinos followed-up by ZTF, **the probability that such a flare should be found by chance is just 0.9%**. It is thus likely that AT2019fdr is indeed the source of IC200530A. AT2019fdr is the first NLS1 flare reported in spatial and temporal coincidence with a high-energy neutrino. However, neutrino emission has been predicted theoretically from Seyfert galaxies [88, see e.g]. Indeed, in light of AT2019dsg, recent theoretical work has suggested that tidal disruption events may share a common neutrino production mechanism with active galaxy cores [89].

[89]: Murase et al. (2020), "High-Energy Neutrino and Gamma-Ray Emission from Tidal Disruption Events"

Observations of AT2019fdr contemporaneous with the neutrino detection are needed to enable comprehensive modelling of the object, and identify possible mechanisms for neutrino production. Radio observations could again reveal the presence of an outflow, found for AT2019dsg and independently proposed for these flares [87]. Such outflows may indeed be the key signature of neutrino production. Conversely, a radio non-detection would strongly disfavour the association of this object with IC200530A.

SN2020xxx

Two likely supernovae were also identified by the pipeline [31], but this is compatible with background expectations, and one has since been firmly excluded as a neutrino counterpart through spectroscopic classification. The other...

SN2019pqh

2.3 Gravitational Waves and Gamma-ray Bursts

In contrast to neutrinos, follow-up of GW and GRB triggers is more akin to searching for a needle in a haystack. The localisations tend to be much larger than for neutrinos, but with the well-defined aim of finding kilonovae. In this case, we at least know what our needle looks like. GW170817 provided an observational confirmation of theoretical predictions of kilonovae, namely that they are faint, fast-evolving, red transients which are generated following mergers of neutron stars. Though a trigger event may cover several hundred or thousand square degrees, these constraints enable us to efficiently reject the vast majority of candidates. Additional temporal coincidence is ensured by requiring that candidates are not detected prior to merger/burst, and spatial coincidence can be ensured using trigger probability skymaps integrated out to predefined confidence intervals (typically 90% or 95%). Unique among triggers, GW events are also typically reported with estimated distance ranges derived from template-matching. For candidates which have a resolved host galaxy, we can determine their distance using spectroscopic surveys such as SDSS, as well as photometric redshift estimates, and veto those candidates lying outside the desired distance range.

The third observing run of the LIGO/VIRGO (O3) extended from X to y, and for this period ZTF has followed-up LVc GW triggers. In this period, there were BNs candidates and Y BBH candidates.

There have been some predictions of EM signatures for BBH events...

Table 2.5: Summary of ZTF follow-up of 13 gravitational wave events in O3. We list the GW False Alarm Rate (FAR) and in parantheses, the probability that the event is terrestrial (P_t). We list the total size of the GW localization region, the GW median distance and the most probable GW classification. We report the integrated probability within the 90% contour of the LALinference skymap, covered by triggered and serendipitous ZTF searches during the first three days after merger observed at least once (P_1), and probability observed at least twice (P_2). In parentheses, we include the coverage based on the BAYESTAR skymap. For some events, only BAYESTAR skymaps were made available. All estimates correct for chip gaps and processing failures. We also report the time lag between merger time and start of ZTF observations (hours), the median depth (AB mag), and the median line-of-sight extinction.

Name	**P_t**	**Area** (sq. deg.)	**Distance** (Mpc)	**Class**	**P_1**	**P_2**	**Time Lag** (hr)	**Depth**	**E(B−V)**
GW190425	1%	7461	156 ± 41	BNS	24.13%	23.90%	0.003	21.5	0.03
S190426c	58%	1131	377 ± 100	NSBH	52.33%	51.57%	13.06	21.5	0.34
S190814bv	1%	23	267 ± 52	NSBH	88.57 %	78.37%	0.00	21.0	0.02
S190901ap	14%	14753	241 ± 79	BNS	56.94%	49.39%	3.61	21.0	0.03
S190910d	2%	2482	632 ± 186	NSBH	32.99%	31.17%	1.51	20.3	0.04
S190910h	39%	24264	230 ± 88	BNS	33.26%	28.92%	0.015	20.4	0.08
S190923y	32%	2107	438 ± 133	NSBH	38.99%	19.22%	13.73	20.1	0.09
S190930t	26%	24220	108 ± 38	NSBH	50.63%	43.42%	11.91	21.1	0.05
S191205ah	7%	6378	385 ± 164	NSBH	5.68%	4.85%	10.66	17.9	0.04
S191213g	23%	4480	201 ± 81	BNS	27.50%	25.10%	0.013	20.4	0.30
S200105ae	97%	7373	283 ± 74	NSBH	52.39%	43.99%	9.96	20.2	0.05
S200115j	1%	765	340 ± 79	NSBH	22.21%	15.76%	0.24	20.8	0.13
S200213t	37%	2326	201 ± 80	BNS	72.17%	70.48%	0.40	21.2	0.19

Conclusion

Appendix

A

TDE Catalogue Results

Table A.1: Summary of the Jetted TDE catalogue.

Source	R.A (deg.)	Dec (deg.)	Distance (Mpc)	T_0 (MJD)	T_1 (MJD)	n_s
Swift J1644+57	251.21	57.58	1909	55644	55749	0.00
Swift J1112-82	167.95	-82.65	5821	55724	55828	0.00
Swift J2058+05	314.58	5.23	8308	55694	55798	1.51

Table A.2: Summary of the Golden TDE catalogue.

Source	R.A (deg.)	Dec (deg.)	Distance (Mpc)	T_0 (MJD)	T_1 (MJD)	n_s
iPTF16fnl	7.49	32.89	72	57600	57730	0.00
XMMSL1 J0740-85	115.03	85.66	76	56718	56848	0.00
ASASSN-15oi	309.79	-30.76	88	57228	57359	0.00
ASASSN-14li	192.06	17.77	91	56851	57072	0.00
ASASSN-14ae	167.17	34.10	195	56658	56851	3.40
PTF09ge	224.26	49.61	290	54953	55083	0.00
iPTF16axa	255.89	30.59	505	57432	57651	0.00
PTF09axc	223.30	22.24	538	55002	55135	0.00
PTF10nuj	246.60	54.71	627	55343	55473	0.47
PS1-10jh	242.37	53.67	826	55326	55470	0.00
PTF09djl	248.48	30.24	904	55020	55150	0.00
PTF11glr	253.53	41.34	1031	55721	55860	0.00
PS1-11af	149.36	3.23	2232	55560	55690	0.00

Table A.3: Summary of the Silver TDE catalogue.

Source	R.A (deg.)	Dec (deg.)	Distance (Mpc)	T_0 (MJD)	T_1 (MJD)	n_s
NGC 247	11.79	-20.76	2	55593	57070	0.00
UGC 03317	83.41	73.72	18	55096	55568	0.00
PGC 1185375	225.96	1.13	23	55228	55358	0.00
PGC 1190358	226.37	1.29	33	55194	55363	0.00
PGC 015259	67.34	-4.76	64	55215	55345	1.48
AT2016ezh	29.52	-0.87	367	57597	57753	0.00
J233454	353.73	14.95	500	55129	55319	1.55
OGLE17aaj	29.10	-71.07	546	57393	57858	0.00
F01004-2237	15.71	-22.37	555	55219	55528	0.00
J094608	146.54	35.21	561	55679	55834	3.51
XJ1500+0154	225.22	1.91	695	54509	54974	0.00
SDSSJ1201	180.40	30.05	700	54992	55457	0.00
CSS100217	157.30	40.71	705	55183	55350	0.00
SN2017bcc	172.97	30.00	711	57802	57938	0.00
DES14C1kia	53.70	-26.33	785	56972	57121	0.32
OGLE16aaa	16.84	-64.27	804	57373	57506	0.00
D23H-1	353.00	0.29	912	54342	54472	1.00
Dougie	182.20	43.02	942	54832	54962	0.00
PS1-10adi	310.69	15.51	1008	55391	55542	0.00
J094806	147.03	3.30	1031	54864	55079	0.57
PTF10iya	219.67	37.66	1127	55323	55453	0.00
ASASSN-15lh	330.56	-61.66	1175	57148	57278	0.00
PS1-13jw	131.22	42.96	1850	56323	56458	0.52
PS1-12yp	202.98	23.90	3447	55933	56126	6.65

Table A.4: Summary of the Obscured TDE catalogue.

Source	R.A (deg.)	Dec (deg.)	Distance (Mpc)	T_0 (MJD)	T_1 (MJD)	n_s
J130819	197.08	43.76	162	54991	55456	7.10
J134244	205.69	5.52	162	54845	55310	0.65
J100933	152.39	23.38	328	54962	55427	0.00
J133737	204.40	20.40	331	54839	55304	0.00
J121116	182.82	0.23	349	54999	55464	0.00
J142401	216.01	29.84	394	54845	55310	0.00
J030257	45.74	-8.50	493	54857	55322	0.00
J141036	212.65	26.91	501	55206	55671	4.87
J113527	173.86	39.47	507	54974	55439	0.00
J145851	224.72	17.85	548	54857	55322	11.88
J133837	204.66	57.52	601	54983	55448	1.39
J155223	238.10	32.58	605	55045	55510	0.63
J091225	138.10	6.17	697	54955	55420	1.09
J123715	189.31	60.20	1083	54967	55432	1.74

B

Neutrino Alerts

Table B.1: Summary of all 67 neutrino alerts issued since 2018 March 20.

Event	R.A. (J2000) [deg]	Dec (J2000) [deg]	90% area [sq. deg.]	Signalness	Ref
IC180423A	-	-	-	-	[56]
IC180908A	144.58	-2.13	6.3	34%	[60]
IC181014A	225.15	-34.80	10.5	-	[61]
IC181023A	270.18	-8.57	9.3	28%	[78]
IC181031A	-	-	-	-	[57]
IC190124A	307.4	-32.18	2.0	-	[62]
IC190205A	-	-	-	-	[58]
IC190221A	268.81	-17.04	5.2	-	[70]
IC190331A	337.68	-20.70	0.4	-	[12]
IC190503A	120.28	+6.35	1.9	36%	[40]
IC190504A	65.7866	-37.44	-	-	[69]
IC190529A	-	-	-	-	[59]
IC190619A	343.26	+10.73	27.2	55%	[42]
IC190629A	27.22	+84.33	-	34%	[71]
IC190704A	161.85	+27.11	21.0	49%	[63]
IC190712A	76.46	+13.06	92.0	30%	[64]
IC190730A	225.79	+10.47	5.4	67%	[13]
IC190819A	148.8	+1.38	9.3	29%	[65]
IC190922A	167.43	-22.39	32.2	20%	[72]
IC190922B	5.76	-1.57	4.5	51%	[17]
IC191001A	314.08	+12.94	25.5	59%	[19]
IC191119A	230.1	+3.17	61.2	45%	[66]
IC191122A	27.25	-0.04	12.2	33%	[73]
IC191204A	79.72	+2.80	11.6	33%	[74]
IC191215A	285.87	+58.92	12.8	47%	[68]
IC191231A	46.36	+20.42	35.6	46%	[75]
IC200107A	148.18	+35.46	7.6	-	[22]
IC200109A	164.49	+11.87	22.5	77%	[49]
IC200117A	116.24	+29.14	2.9	38%	[51]

Event	R.A. (J2000) [deg]	Dec (J2000) [deg]	90% area [sq. deg.]	Signalness	Ref
IC200120A	-	-	-	-	[76]
IC200227A	348.26	+21.32	-	35%	[67]
IC200410A	242.58	+11.61	377.9	31%	[81]
IC200421A	87.93	+8.23	24.4	33%	[79]
IC200425A	100.1	+53.57	18.8	48%	[82]
IC200512A	295.18	+15.79	9.8	32%	[54]
IC200523A	338.64	+1.75	90.6	25%	[83]
IC200530A	255.37	+26.61	25.3	59%	[30]
IC200614A	33.84	+31.61	47.8	42%	[84]
IC200615A	142.95	+3.66	5.9	83%	[80]
IC200620A	162.11	+11.95	1.7	32%	[55]
IC200728A	-	-	-	-	**[ic200728a]**
IC200806A	157.25	+47.75	1.8	40%	**[ic200806a]**
IC200911A	51.11	+38.11	52.7	41%	**[ic200911a]**
IC200916A	109.78	+14.36	4.2	32%	**[ic200916a]**
IC200921A	195.29	+26.24	12.0	41%	**[ic200921a]**
IC200926A	96.46	-4.33	1.7	44%	**[ic200926a]**
IC200926B	184.75	+32.93	9.0	43%	**[ic200926b]**
IC200929A	29.53	+3.47	1.1	47%	**[ic200929a]**
IC201007A	265.17	+5.34	0.6	88%	**[ic201007a]**
IC201014A	221.22	+14.44	1.9	41%	**[ic201014a]**
IC201021A	260.82	+14.55	6.9	30%	**[ic201021a]**
IC201114A	105.25	+6.05	4.5	56%	**[ic201114a]**
IC201115A	195.12	+1.38	6.6	46%	**[ic201115a]**
IC201115B	-	-	-	-	**[ic201115b]**
IC201120A	307.53	+40.77	64.3	50%	**[ic201120a]**
IC201130A	30.54	-12.10	5.4	15%	**[ic201130a]**
IC201209A	6.86	-9.25	4.7	19%	**[ic201209a]**
IC201221A	261.69	+41.81	8.9	56%	**[ic201221a]**
IC201222A	206.37	+13.44	1.5	53%	**[ic201222a]**
IC210210A	206.06	+4.78	2.8	65%	**[ic210210a]**
IC210213A	-	-	-	-	**[ic210213a]**
IC210322A	-	-	-	-	**[ic210322a]**
IC210503A	143.53	+41.81	102.6	41%	**[ic210503a]**
IC210510A	268.42	+3.81	4.0	28%	**[ic210510a]**
IC210516A	91.76	+9.52	2.2	29%	**[ic210516a]**
IC210519A	-	-	-	-	**[ic210519a]**
IC210608A	337.41	+18.37	109.7	31%	**[ic210608a]**

Bibliography

Here are the references in citation order.

[1] M. G. Aartsen et al. "The IceCube realtime alert system." In: *Astroparticle Physics* 92 (June 2017), pp. 30–41. DOI: 10.1016/j.astropartphys.2017.05.002 (cited on pages 6, 9).

[2] M. G. Aartsen et al. "Constraints on Ultrahigh-Energy Cosmic-Ray Sources from a Search for Neutrinos above 10 PeV with IceCube." In: P*hys. Rev. Lett.* 117.24, 241101 (Dec. 2016), p. 241101. DOI: 10.1103/PhysRevLett.117.241101 (cited on page 6).

[3] M. G. Aartsen et al. "Observation of High-Energy Astrophysical Neutrinos in Three Years of IceCube Data." In: P*hys. Rev. Lett.* 113.10, 101101 (Sept. 2014), p. 101101. DOI: 10.1103/PhysRevLett.113.101101 (cited on page 6).

[4] E. Blaufuss et al. "The Next Generation of IceCube Real-time Neutrino Alerts." In: *36th International Cosmic Ray Conference (ICRC2019)*. Vol. 36. International Cosmic Ray Conference. July 2019, 1021, p. 1021 (cited on pages 6, 9, 19).

[5] Thomas Kintscher. "Rapid Response to Extraordinary Events: Transient Neutrino Sources with the IceCube Experiment." PhD thesis. Humboldt-Universität zu Berlin, Mathematisch-Naturwissenschaftliche Fakultät, 2020. DOI: http://dx.doi.org/10.18452/21948 (cited on page 6).

[6] Pan-Starrs Collaboration et al. "Search for transient optical counterparts to high-energy IceCube neutrinos with Pan-STARRS1." In: A*&A* 626, A117 (June 2019), A117. DOI: 10.1051/0004-6361/201935171 (cited on pages 7, 9).

[7] Christian Haack and Christopher Wiebusch. "A measurement of the diffuse astrophysical muon neutrino flux using eight years of IceCube data." In: *PoS* ICRC2017 (2017), p. 1005. DOI: 10.22323/1.301.1005 (cited on page 8).

[8] E. Blaufuss. "ICECUBE-160427A neutrino candidate event: updated direction information." In: *GRB Coordinates Network* 19363 (Jan. 2016), p. 1 (cited on page 9).

[9] C. Kopper and E. Blaufuss. "IceCube-170922A - IceCube observation of a high-energy neutrino candidate event." In: *GRB Coordinates Network* 21916 (Jan. 2017), p. 1 (cited on page 10).

[10] Yasuyuki T. Tanaka, Sara Buson, and Daniel Kocevski. "Fermi-LAT detection of increased gamma-ray activity of TXS 0506+056, located inside the IceCube-170922A error region." In: *The Astronomer's Telegram* 10791 (Sept. 2017), p. 1 (cited on page 10).

[11] IceCube Collaboration et al. "Multimessenger observations of a flaring blazar coincident with high-energy neutrino IceCube-170922A." In: *Science* 361.6398, eaat1378 (July 2018), eaat1378. DOI: 10.1126/science.aat1378 (cited on page 10).

[12] C. Kopper. "IceCube-190331A - IceCube observation of a high-energy neutrino candidate event." In: *GRB Coordinates Network* 24028 (Mar. 2019), p. 1 (cited on pages 10, 20, 21, 33).

[13] R. Stein. "IceCube-190730A - IceCube observation of a high-energy neutrino candidate event." In: *GCN Circular* 25225 (July 2019) (cited on pages 11, 20, 33).

[14] A. Franckowiak et al. "Patterns in the Multiwavelength Behavior of Candidate Neutrino Blazars." In: A*pJ* 893.2, 162 (Apr. 2020), p. 162. DOI: 10.3847/1538-4357/ab8307 (cited on page 11).

[15] S. Kiehlmann et al. "Neutrino candidate source FSRQ PKS 1502+106 at highest flux density at 15 GHz." In: *The Astronomer's Telegram* 12996 (Aug. 2019), p. 1 (cited on page 11).

[16] Xavier Rodrigues et al. "Multiwavelength and Neutrino Emission from Blazar PKS 1502 + 106." In: A*pJ* 912.1, 54 (May 2021), p. 54. DOI: 10.3847/1538-4357/abe87b (cited on page 11).

[17] Erik Blaufuss. "IceCube-190922B - IceCube observation of a high-energy neutrino candidate event." In: *GCN Circular* 25806 (Sept. 2019) (cited on pages 11, 20, 33).

[18] Robert Stein et al. “A candidate supernova coincident with IceCube-190922B from ZTF.” In: *The Astronomer’s Telegram* 13125 (Sept. 2019), p. 1 (cited on pages 11, 20).

[19] R. Stein. “IceCube-191001A - IceCube observation of a high-energy neutrino candidate event.” In: *GCN Circular* 25913 (Oct. 2019) (cited on pages 11, 20, 33).

[20] Robert Stein et al. “A tidal disruption event coincident with a high-energy neutrino.” In: *Nature Astronomy* (Feb. 2021). DOI: 10.1038/s41550-020-01295-8 (cited on page 11).

[21] Sjoert van Velzen et al. “Seventeen Tidal Disruption Events from the First Half of ZTF Survey Observations: Entering a New Era of Population Studies.” In: *arXiv e-prints*, arXiv:2001.01409 (Jan. 2020), arXiv:2001.01409 (cited on page 12).

[22] R. Stein. “IceCube-200107A: IceCube observation of a high-energy neutrino candidate event.” In: *GCN Circular* 26655 (Jan. 2020) (cited on pages 12, 19, 20, 33).

[23] M. Kronmueller and T. Glauch. “Application of Deep Neural Networks to Event Type Classification in IceCube.” In: *36th International Cosmic Ray Conference (ICRC2019)*. Vol. 36. International Cosmic Ray Conference. July 2019, 937, p. 937 (cited on page 12).

[24] P. Padovani et al. “Extreme blazars as counterparts of IceCube astrophysical neutrinos.” In: *MNRAS* 457.4 (Apr. 2016), pp. 3582–3592. DOI: 10.1093/mnras/stw228 (cited on page 12).

[25] F. Krauss et al. “Swift follow-up observations of IceCube-200107A: Identification of a X-ray high state for 4FGL J0955.1+3551.” In: *The Astronomer’s Telegram* 13395 (Jan. 2020), p. 1 (cited on page 12).

[26] P. Giommi, T. Glauch, and E. Resconi. “Swift observation of a flaring very extreme blazar in the error region of the high-energy neutrino Ice-Cube 200107A.” In: *The Astronomer’s Telegram* 13394 (Jan. 2020), p. 1 (cited on page 12).

[27] Vaidehi S. Paliya et al. “Multifrequency Observations of the Candidate Neutrino-emitting Blazar BZB J0955+3551.” In: *ApJ* 902.1, 29 (Oct. 2020), p. 29. DOI: 10.3847/1538-4357/abb46e (cited on page 12).

[28] P. Giommi et al. “3HSP J095507.9+355101: A flaring extreme blazar coincident in space and time with IceCube-200107A.” In: *A&A* 640, L4 (Aug. 2020), p. L4. DOI: 10.1051/0004-6361/202038423 (cited on page 12).

[29] Maria Petropoulou et al. “Comprehensive Multimessenger Modeling of the Extreme Blazar 3HSP J095507.9+355101 and Predictions for IceCube.” In: *ApJ* 899.2, 113 (Aug. 2020), p. 113. DOI: 10.3847/1538-4357/aba8a0 (cited on page 12).

[30] R. Stein. “IceCube-200530A: IceCube observation of a high-energy neutrino candidate event.” In: *GCN Circular* 27865 (2020) (cited on pages 12, 19, 20, 34).

[31] S. Reusch et al. “IceCube-200530A: Candidate Counterparts from the Zwicky Transient Facility.” In: *GCN Circular* 27872 (May 2020) (cited on pages 12, 19, 20, 23).

[32] Sara Frederick et al. “A Family Tree of Optical Transients from Narrow-Line Seyfert 1 Galaxies.” In: *arXiv e-prints*, arXiv:2010.08554 (Oct. 2020), arXiv:2010.08554 (cited on page 12).

[33] Eric C. Bellm et al. “The Zwicky Transient Facility: Surveys and Scheduler.” In: *PASP* 131.1000 (June 2019), p. 068003. DOI: 10.1088/1538-3873/ab0c2a (cited on page 17).

[34] Michael W. Coughlin et al. “2900 Square Degree Search for the Optical Counterpart of Short Gamma-Ray Burst GRB 180523B with the Zwicky Transient Facility.” In: *PASP* 131.998 (Apr. 2019), p. 048001. DOI: 10.1088/1538-3873/aaff99 (cited on page 18).

[35] J. Nordin et al. “Transient processing and analysis using AMPEL: alert management, photometry, and evaluation of light curves.” In: *A&A* 631, A147 (Nov. 2019), A147. DOI: 10.1051/0004-6361/201935634 (cited on page 18).

[36] Ashish Mahabal et al. “Machine Learning for the Zwicky Transient Facility.” In: *PASP* 131.997 (Mar. 2019), p. 038002. DOI: 10.1088/1538-3873/aaf3fa (cited on page 18).

[37] Gaia Collaboration et al. “Gaia Data Release 2. Summary of the contents and survey properties.” In: *A&A* 616, A1 (Aug. 2018), A1. DOI: 10.1051/0004-6361/201833051 (cited on page 18).

[38] Yutaro Tachibana and A. A. Miller. "A Morphological Classification Model to Identify Unresolved PanSTARRS1 Sources: Application in the ZTF Real-time Pipeline." In: P*ASP* 130.994 (Dec. 2018), p. 128001. DOI: 10.1088/1538-3873/aae3d9 (cited on page 18).

[39] Edward L. Wright et al. "The Wide-field Infrared Survey Explorer (WISE): Mission Description and Initial On-orbit Performance." In: A*J* 140.6 (Dec. 2010), pp. 1868–1881. DOI: 10.1088/0004-6256/140/6/1868 (cited on page 18).

[40] E. Blaufuss. "IceCube-190503A - IceCube observation of a high-energy neutrino candidate event." In: *GCN Circular* 24378 (May 2019) (cited on pages 20, 33).

[41] R. Stein et al. "Optical follow-up of IceCube-190503A with ZTF." In: *The Astronomer's Telegram* 12730 (May 2019), p. 1 (cited on page 20).

[42] E. Blaufuss. "IceCube-190619A - IceCube observation of a high-energy neutrino candidate event." In: *GCN Circular* 24854 (June 2019) (cited on pages 20, 33).

[43] R. Stein et al. "Optical follow-up of IceCube-190619A with ZTF." In: *The Astronomer's Telegram* 12879 (June 2019), p. 1 (cited on page 20).

[44] R. Stein et al. "Optical follow-up of IceCube-190730A with ZTF." In: *The Astronomer's Telegram* 12974 (July 2019), p. 1 (cited on page 20).

[45] Robert Stein et al. "IceCube-190922B: Identification of a Candidate Supernova from the Zwicky Transient Facility." In: *GCN Circular* 25824 (2019) (cited on page 20).

[46] Robert Stein et al. "Candidate Counterparts to IceCube-191001A with ZTF." In: *The Astronomer's Telegram* 13160 (Oct. 2019), p. 1 (cited on page 20).

[47] Robert Stein et al. "IceCube-191001A: Candidate Counterparts with the Zwicky Transient Facility." In: *GCN Circular* 25929 (2019) (cited on page 20).

[48] Robert Stein and Simeon Reusch. "IceCube-200107A: No candidates from the Zwicky Transient Facility." In: *GCN Circular* 26667 (Jan. 2020) (cited on page 20).

[49] R. Stein. "IceCube-200109A: IceCube observation of a high-energy neutrino candidate event." In: *GCN Circular* 26696 (Jan. 2020) (cited on pages 20, 33).

[50] Simeon Reusch and Robert Stein. "IceCube-200109A: Candidate Counterparts from the Zwicky Transient Facility." In: *GCN Circular* 26747 (Jan. 2020) (cited on page 20).

[51] C. Lagunas Gualda. "IceCube-200117A: IceCube observation of a high-energy neutrino candidate event." In: *GCN Circular* 26802 (Jan. 2020) (cited on pages 20, 33).

[52] Simeon Reusch and Robert Stein. "IceCube-200117A: Candidate Counterpart from the Zwicky Transient Facility." In: *GCN Circular* 26813 (Jan. 2020) (cited on page 20).

[53] Simeon Reusch and Robert Stein. "IceCube-200117A: One Additional Candidate Counterpart from the Zwicky Transient Facility." In: *GCN Circular* 26816 (Jan. 2020) (cited on page 20).

[54] C. Lagunas Gualda. "IceCube-200512A: IceCube observation of a high-energy neutrino candidate event." In: *GCN Circular* 27719 (May 2020) (cited on pages 20, 34).

[55] M. Santander. "IceCube-200620A: IceCube observation of a high-energy neutrino candidate event." In: *GCN Circular* 27997 (June 2020) (cited on pages 20, 34).

[56] C. Kopper. "Retraction of IceCube GCN/AMON NOTICE 71165249_130949." In: *GCN Circular* 22669 (Apr. 2018) (cited on pages 20, 21, 33).

[57] E. Blaufuss. "IceCube-181031A retraction." In: *GCN Circular* 23398 (Oct. 2018) (cited on pages 20, 21, 33).

[58] E. Blaufuss. "Retraction of IceCube GCN/AMON NOTICE 36142391_132143." In: *GCN Circular* 23876 (Feb. 2019) (cited on pages 20, 21, 33).

[59] E. Blaufuss. "IceCube 41485283_132628.amon retraction." In: *GCN Circular* 24674 (May 2019) (cited on pages 20, 21, 33).

[60] E. Blaufuss. "IceCube-180908A - IceCube observation of a high-energy neutrino candidate event." In: *GCN Circular* 23214 (Sept. 2018) (cited on pages 20, 21, 33).

[61] I. Taboada. "IceCube-181014A - IceCube observation of a high-energy neutrino candidate event." In: *GCN Circular* 23338 (Oct. 2018) (cited on pages 20, 21, 33).

[62] E. Blaufuss. "IceCube-190124A - IceCube observation of a high-energy neutrino candidate event." In: *GCN Circular* 23785 (Jan. 2019) (cited on pages 20, 21, 33).

[63] M. Santander. "IceCube-190704A - IceCube observation of a high-energy neutrino candidate event." In: *GCN Circular* 24981 (July 2019) (cited on pages 20, 21, 33).

[64] E. Blaufuss. "IceCube-190712A - IceCube observation of a high-energy neutrino candidate event." In: *GCN Circular* 25057 (July 2019) (cited on pages 20, 21, 33).

[65] M. Santander. "IceCube-190819A - IceCube observation of a high-energy neutrino candidate event." In: *GCN Circular* 25402 (Aug. 2019) (cited on pages 20, 21, 33).

[66] E. Blaufuss. "IceCube-191119A - IceCube observation of a high-energy neutrino candidate event." In: *GCN Circular* 26258 (Nov. 2019) (cited on pages 20, 21, 33).

[67] R. Stein. "IceCube-200227A: IceCube observation of a high-energy neutrino candidate event." In: *GCN Circular* 27235 (Feb. 2020) (cited on pages 20, 21, 34).

[68] R. Stein. "IceCube-191215A - IceCube observation of a high-energy neutrino candidate event." In: *GCN Circular* 26435 (Dec. 2019) (cited on pages 20, 21, 33).

[69] C. Kopper. "IceCube-190504A - IceCube observation of a high-energy neutrino candidate event." In: *GCN Circular* 24392 (May 2019) (cited on pages 20, 21, 33).

[70] I. Taboada. "IceCube-190921A - IceCube observation of a high-energy neutrino candidate event." In: *GCN Circular* 23918 (Feb. 2019) (cited on pages 20, 21, 33).

[71] E. Blaufuss. "IceCube-190629A - IceCube observation of a high-energy neutrino candidate event." In: *GCN Circular* 24910 (June 2019) (cited on pages 20, 21, 33).

[72] R. Stein. "IceCube-190922A - IceCube observation of a high-energy neutrino candidate event." In: *GCN Circular* 25802 (Sept. 2019) (cited on pages 20, 21, 33).

[73] E. Blaufuss. "IceCube-191122A - IceCube observation of a high-energy neutrino candidate event." In: *GCN Circular* 26276 (Nov. 2019) (cited on pages 20, 21, 33).

[74] R. Stein. "IceCube-191204A - IceCube observation of a high-energy neutrino candidate event." In: *GCN Circular* 26341 (Dec. 2019) (cited on pages 20, 21, 33).

[75] M. Santander. "IceCube-191231A: IceCube observation of a high-energy neutrino candidate event." In: *GCN Circular* 26620 (Dec. 2019) (cited on pages 20, 21, 33).

[76] C. Lagunas Gualda. "IceCube-200120A: IceCube observation of a high-energy neutrino candidate event." In: *GCN Circular* 26832 (Jan. 2020) (cited on pages 20, 21, 34).

[77] E. Blaufuss. "IceCube-200120A: Event likely due to background." In: *GCN Circular* 26874 (Jan. 2020) (cited on page 20).

[78] E. Blaufuss. "IceCube-181023A - IceCube observation of a high-energy neutrino candidate event." In: *GCN Circular* 23375 (Oct. 2018) (cited on pages 20, 21, 33).

[79] E. Blaufuss. "IceCube-200415A: IceCube observation of a high-energy neutrino candidate event." In: *GCN Circular* 27612 (Apr. 2020) (cited on pages 21, 34).

[80] C. Lagunas Gualda. "IceCube-200615A: IceCube observation of a high-energy neutrino candidate event." In: *GCN Circular* 27950 (June 2020) (cited on pages 21, 34).

[81] R. Stein. "IceCube-200410A: IceCube observation of a high-energy neutrino candidate event." In: *GCN Circular* 27534 (Apr. 2020) (cited on pages 21, 34).

[82] M. Santander. "IceCube-200425A: IceCube observation of a high-energy neutrino candidate event." In: *GCN Circular* 27651 (Apr. 2020) (cited on pages 21, 34).

[83] E. Blaufuss. "IceCube-200523A: IceCube observation of a high-energy neutrino candidate event." In: *GCN Circular* 27787 (May 2020) (cited on pages 21, 34).

[84] E. Blaufuss. "IceCube-200614A: IceCube observation of a high-energy neutrino candidate event." In: *GCN Circular* 27941 (June 2020) (cited on pages 21, 34).

[85] J. Nordin et al. "ZTF Transient Discovery Report for 2019-05-13." In: *Transient Name Server Discovery Report* 2019-771 (May 2019), p. 1 (cited on page 21).

[86] R. Chornock et al. "Transient Classification Report for 2019-06-15." In: *Transient Name Server Classification Report* 2019-1016 (June 2019), p. 1 (cited on page 22).

[87] B. Trakhtenbrot et al. "A new class of flares from accreting supermassive black holes." In: *Nature Astronomy* 3 (Jan. 2019), pp. 242–250. DOI: 10.1038/s41550-018-0661-3 (cited on page 22).

[88] K. Murase. "Active Galactic Nuclei as High-Energy Neutrino Sources." In: *Neutrino Astronomy: Current Status, Future Prospects*. Ed. by Thomas Gaisser and Albrecht Karle. 2017, pp. 15–31. DOI: 10.1142/9789814759410_0002 (cited on page 22).

[89] K. Murase et al. "High-Energy Neutrino and Gamma-Ray Emission from Tidal Disruption Events." In: *arXiv e-prints*, arXiv:2005.08937 (May 2020) (cited on page 22).

Alphabetical Index